macromol

MDPI

Article

Fluorescent Hyperbranched Polymers and Cotton Fabrics Treated with Them as Innovative Agents for Antimicrobial Photodynamic Therapy and Self-Disinfecting Textiles

Desislava Staneva [1,*], Paula Bosch [2], Petar Grozdanov [3], Ivanka Nikolova [3] and Ivo Grabchev [4,*]

[1] Department of Textile, Leather and Fuels, University of Chemical Technology and Metallurgy, 1756 Sofia, Bulgaria
[2] Institute of Science and Technology of Polymers, Spanish National Research Council (ICTP-CSIC), 28006 Madrid, Spain; pbosch@ictp.csic.es
[3] The Stephan Angeloff Institute of Microbiology, Bulgarian Academy of Sciences, 1113 Sofia, Bulgaria; grozdanov@microbio.bas.bg (P.G.); vanianik@mail.bg (I.N.)
[4] Faculty of Medicine, Sofia University "St. Kliment Ohridski", 1407 Sofia, Bulgaria
* Correspondence: grabcheva@mail.bg (D.S.); i.grabchev@chem.uni-sofia.bg (I.G.)

Abstract: The results of this study, which involved treating cotton fabrics with three fluorescent hyperbranched polymers modified with 1,8-naphthalamide (P1), acridine (P2), and dansyl (P3) groups, could have applications in the development of antimicrobial textiles with self-disinfecting ability. The polymers, dissolved in DMF/water solution, were deposited on the cotton fabric using the exhaustion method. The fabrics were thoroughly analyzed by reflection spectra, CIEL*a*b* coordinates, and color difference (ΔE). The release of the polymers from the cotton surface was studied in a phosphate buffer with pH = 7.4 and an acetate buffer with pH = 4.5 at 37 °C for 10 h. It is shown that at pH = 7.4, the release of the three polymers occurs slowly (about 4–5%). In contrast, in an acidic medium, due to protonation of the tertiary amino group of 1,8-naphthalimide, P1 passes significantly more readily into the aqueous solution (35%). The possibility of singlet oxygen ($^1O_2$) generation by the polymers and the cotton fabrics treated with them under sunlight irradiation was followed using an iodometric method. The microbiological activity was investigated against Gram-positive *Bacillus cereus* and Gram-negative *Pseudomonas aeruginosa* as model bacterial strains in the dark and after irradiation with sunlight. The antimicrobial activity of the polymers increased after light irradiation, as $^1O_2$ attacks and destroys the bacterial cell membrane. Scanning electron microscopy showed that a stable bacterial biofilm had formed on the untreated cotton surface, but treatment with hyperbranched polymers prevented its formation. However, many bacteria were still observed on the fiber surface when the microbial test was performed in the dark, whereas only a few single bacteria were noticed after the illumination. A virucidal effect against respiratory viruses HRSV-2 and AAdV-5 was observed only after irradiation with sunlight.

Keywords: hyperbranched polymers; cotton; antimicrobial photodynamic therapy; singlet oxygen; virucidal

check for updates

Academic Editor: Ana María Díez-Pascual

Received: 17 March 2025
Revised: 29 May 2025
Accepted: 10 June 2025
Published: 11 June 2025

Citation: Staneva, D.; Bosch, P.; Grozdanov, P.; Nikolova, I.; Grabchev, I. Fluorescent Hyperbranched Polymers and Cotton Fabrics Treated with Them as Innovative Agents for Antimicrobial Photodynamic Therapy and Self-Disinfecting Textiles. *Macromol* **2025**, *5*, 26. https://doi.org/10.3390/macromol5020026

Copyright: © 2025 by the authors. Licensee MDPI, Basel, Switzerland. This article is an open access article distributed under the terms and conditions of the Creative Commons Attribution (CC BY) license (https://creativecommons.org/licenses/by/4.0/).

1. Introduction

In recent years, infectious diseases have become one of the leading causes of mortality in the world due to the weak antibiotic effect of the medications used in clinical practice against pathogenic microorganisms [1–4]. As a result, difficult-to-treat infections arise, which is why, according to the World Health Organization, we are about to enter

the so-called "post-antibiotic era." [5]. Searching, developing, and implementing new highly effective agents with microbiological activity is necessary to overcome this. To effectively combat antibiotic resistance, it is essential to expand the understanding of this multifaceted phenomenon by clarifying the fundamental mechanisms and interactions between antibiotic-resistant bacterial cells and how antibiotics are used. The search for new strategies to stop the increase in antibiotic resistance is considered to be of crucial importance. The use of photoactive compounds, called photosensitizers (PS), gives a new impetus to the study of the enhancement of their activity after irradiation with light and the application of antimicrobial photodynamic therapy (APDT) [6,7]. This new, promising strategy can be applied to inactivating a wide range of pathogenic bacteria, especially those that form stable biofilms [8,9]. Biofilm formation is a multistep process, and the mechanisms for its appearance and development involve (i) bacterial attachment, (ii) maturation, and (iii) bacterial release [10]. Therefore, the antimicrobial effectiveness for the infection's spreading protection and emergence of drug-resistant microbes depends on counteracts to each step of its formation [11].

Antiviral drug resistance is also a concern, similarly to antibiotic resistance. In recent years, the spread of dangerous viruses, such as coronaviruses SARS-CoV, SARS-CoV-2, MERS-CoV, filovirus Ebola, and seasonal respiratory viruses, intensified the research on discovering and developing new therapeutic effective agents [12]. The viruses' resistance appears as they evolve into new variants and sub-variants due to the accumulation of mutations in the genomes during their replication in the human body or as a result of recombination between several simultaneously circulating viral strains. As in treating bacteria, photodynamic virus inactivation can be considered an alternative path in antiviral treatments without resistance formation. The photosensitizers used in vitro and in vivo have different chemical structures, which absorb in a wide spectral range from the ultraviolet to the near-infrared region [13]. Their multi-target mode of action can explain the observed resistance decrease [14,15].

Fabric modification with antimicrobial substances is one of the methods for obtaining materials that can inhibit or destroy the growth of microorganisms and prevent biofilm formation on the surface of textile fibers [16,17]. The photosensitizer applied on the fiber surface is the way to obtain self-disinfecting textiles. Such materials can be considered successful tools for prevention of microorganisms and managing infectious diseases.

In recent years, our laboratory has conducted extensive and systematic scientific research on synthesizing dendrimers emitting fluorescence with different colors and intensities and their metal complexes [18,19]. The presence of several fluorophores in one macromolecule increases the biological activity of the tested substances, reducing the required concentration of an antimicrobial that will inhibit the visible growth of a microorganism or minimum inhibitory concentrations (MICs). A new promising trend for enhancement of their microbiological activity is designing systems with the synergistic effect between the active polymer components as an antibiofilm-forming agent and their ability to produce reactive oxygen species upon irradiation with light [20,21]. Their activity is preserved after surface treatment on cotton fabric, resulting in antimicrobial and self-disinfecting properties [22]. In the dark, the immobilized antimicrobial compounds on the fiber surface prevent bacteria's attachment, aggregation, and spreading. The released singlet oxygen further attacks bacteria cells, disturbs the biofilm architecture, and prevents its formation.

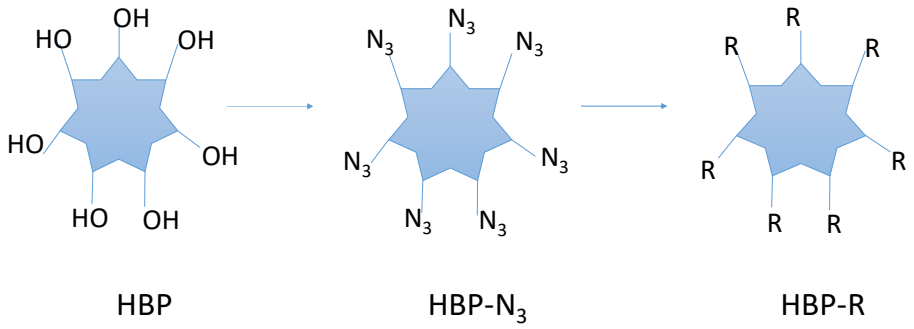
Unlike dendrimers, the other highly branched macromolecules with many reactive functional groups are three-dimensional hyperbranched polymers that are characterized by low viscosity and good solubility in organic solvents. They do not have perfect structure like dendrimers, but they are significantly cheaper and can also be used as a matrix for

covalent binding with different fluorophores. We recently described the modification of hyperbranched polymers with 1,8-naphthalimide (P1) [23], acridine (P2) [24], and dansyl (P3) [25] groups by the click chemistry method and investigated their photophysical properties in organic solvents. We also investigated the dark microbiological activity of the three polymers against Gram-positive and Gram-negative bacteria and fungi [25–27]. The good results obtained and the photoactivity of these polymers prompted us to continue examining light's influence on their antimicrobial activity.

This work presents the results of the first use of hyperbranched photoactive polymers as photodynamic antibacterial agents in solution and after their application on cotton fabric against Gram-positive and *Bacillus cereus* and Gram-negative *Pseudomonas aeruginosa* as model bacterial strains and two respiratory viruses, HRSV-2 and HAdV-5. The generation of singlet oxygen and its role in the inactivation of the growth of pathogenic microorganisms are described.

2. Materials and Methods

The synthesis and spectral properties of the hyperbranched polymers modified with photoactive fluorophores as 1,8-naphthalimide (P1), acridine (P2), and dansyl (P3) have been described (Scheme 1). The hyperbranched polymer P1000 (HBP) with a molecular weight m = 1185 g mol^{-1} has seven reactive hydroxyl groups, which are transformed into azido groups, resulting in an azido-functionalized hyperbranched polymer (HBP-N3). These functional groups react with the previously acetylene-functionalized fluorophores via a Husgen 1,3 dipolar cycloaddition (Scheme 1). The click reaction between (HBP-N3) and the fluorophores was conducted at room temperature for 24 h. NMR and elemental analysis revealed that six fluorophores are chemically bound to the polymer molecule. The proposed chemical structure of the hyperbranched polymers is shown in Scheme 2 [23–25].

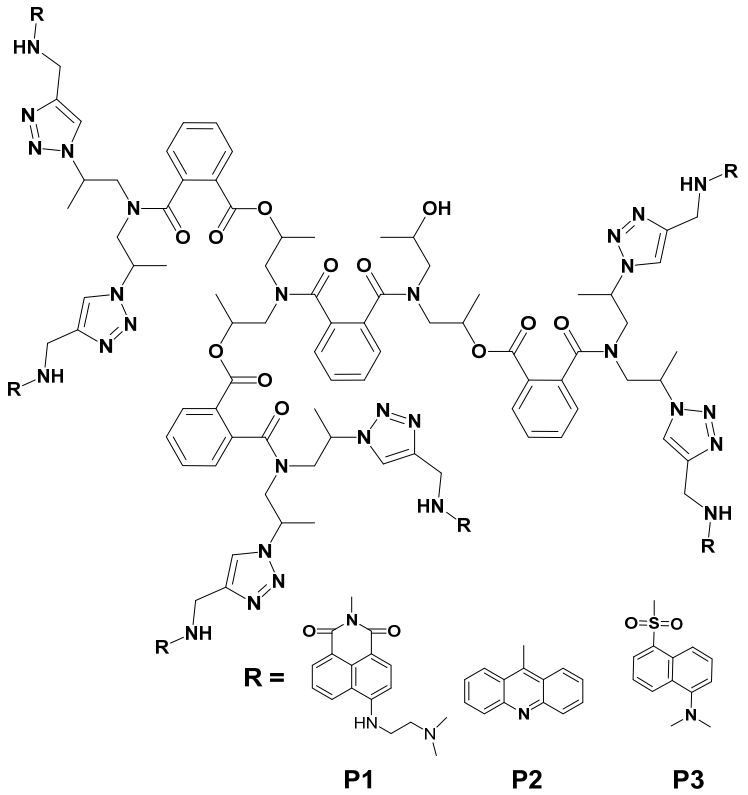


Scheme 1. Synthetic route of hyperbranched polymers P1–P3.

Unbleached 100% cotton fabric (weight per unit area of 140 g m^{-2}) was used. Potassium iodide for analysis (Merck, Darmstadt, Germany), phosphate-buffer solution (1.0 M, pH = 7.4) (Merck, Germany), and Sodium acetate buffer solution (1.0 M, pH = 4.5) (Fisher Chemical, Schwerte, Germany) were used.

The UV-Arian Cary 5000 UV-Vis-NIR spectrophotometer (Agilent Technologies Inc., Santa Clara, CA, USA) and Cary Eclipse spectrofluorometer (Agilent Technologies Inc., Santa Clara, CA, USA) have been used to record absorption and fluorescence spectra.

Color measurements of the fabrics modified with polymers P1–P3 were determined using a Konica Minolta CM-36dG spectrophotometer (Konica Minolta, Inc., Tokyo, Japan). The light source was D65. It simulates average daylight with a color temperature of 6500K, including ultraviolet wavelength region. The illumination-observation geometry was D/10°.



Scheme 2. Chemical structure of modified photoactive hyperbranched polymers P1–P3.

2.1. Treatment of Cotton Fabric with Polymers P1–P3 and Color Measurements

A total of 5 mg of P1–P3 polymers was dissolved in 1 mL of DMF, and the solution was added to 50 mL of deionised water. A total of 1 g of cotton fabric was added to the resulting fine emulsion, and the temperature was increased to 60 °C for 3 h of stirring. After that, the fabric was removed, dried at room temperature, washed with water, and dried again at room temperature. The number of deposited polymers was determined by measuring the fluorescence intensity of the solutions before and after treatment of the cotton fabric with them.

The colors of the obtained three fabrics were evaluated in the Commission Internationale de l'Elcairage (CIE) space by three coordinates L* (lightness), a* (transition from green (−a*) to red (+a*)), and b* (transition from blue (−b*) to yellow (+b*)), that are calculated with Equations (1)–(3):

$$L^* = 116\,(Y/Y_0)^{1/3} - 16 \quad (1)$$

$$a^* = 500\,[(X/X_0)^{1/3} - (Y/Y_0)^{1/3}] \quad (2)$$

$$b^* = 200\,[(Y/Y_0)^{1/3} - (Z/Z_0)^{1/3}]. \quad (3)$$

X_0, Y_0, and Z_0 are the tristimulus values of a particular achromatic light used in illumination, and X, Y, and Z are the values defined for colored fabrics. The Y_0 values are normalized such that $Y_0 = 100$.

The color difference ΔE* is used to quantify the visually detectable color changes in the obtained fabrics compared with untreated fabric and can be calculated by Equation (4):

$$\Delta E^* = [(\Delta L^*)^2 + (\Delta a^*)^2 + (\Delta b^*)^2]^{1/2}, \quad (4)$$

where ΔL*, Δa*, and Δb*are the differences in the coordinates of the control untreated cotton fabric and the P1–P3 treated fabrics.

2.2. The Release of Polymers P1–P3 from the Cotton Surface

The release of the polymers from the cotton fabric with a size of (2.0 cm × 2.0 cm) was studied in a phosphate buffer with pH = 7.4 and an acetate buffer with pH = 4.5 at 37 °C. The solution's fluorescence intensity was measured every 1 h for 10 h.

2.3. Iodometric Measurements

KI (0.5 M) was added to the aqueous solutions (20 mL) of each of the polymers P1–P3 with a concentration of c = 1×10^{-6} M. Each solution was illuminated with sunlight using a Newport solar simulator: 150 W Xe, (36 mW cm^{-1}). The 1 cm^2 of P1–P3-treated cotton fabrics were placed in 20 mL of KI (0.5 M) solution and irradiated similarly to the dissolved polymers with stirring. The lamp and the tube were at a distance of 25 cm from each other. Irradiated aqueous solutions (3 mL) were placed in a quartz cuvette, and their absorption spectra were recorded in the range from 250 to 500 nm. After this measurement, the solutions were added to the stock solution, and irradiation continued for 60 min.

2.4. In Vitro Antimicrobial Assay

The antimicrobial activity of P1–P3 was tested against Gram-positive *Bacillus cereus* (ATCC11778) and Gram-negative *Pseudomonas aeruginosa* (1390) as model bacterial strains, which were maintained on meat-peptone agar (MPA) slants and transferred monthly at 4 °C. The ability of polymers P1–P3 to inhibit the growth of the model strains was tested in meat-peptone broth (MPB) in dark and under light illumination. The compounds were dissolved in DMSO at a started concentration of 1.0 mg ml^{-1} and further diluted in test tubes with meat-peptone broth (MPB) to final concentrations of 50, 40, 25, and 10 μg mL^{-1}. The tubes were inoculated and then incubated for 18 h at appropriate temperatures in light and dark. Negative controls (MPB and inoculum, without compounds) and Positive controls (compound and meat-peptone broth, without inoculum) were also prepared. The microbial growth was tested by measuring each tube's optical density at 600 nm (OD_{600}). The microbial growth (in%) was determined based on the positive control (considered as 100%). The experiments were conducted in triplicate, and the averages (standard deviations of less than 5%) were taken.

2.5. Antimicrobial Assay of Modified Cotton Fabrics

The antimicrobial activity of the cotton fabrics treated with polymers was tested in MPB against the model strains under light irradiation and in the dark. Tubes containing MPB and square-shaped cotton samples (1.0 cm × 1.0 cm) were inoculated with the standardized microbial suspension. Tubes with native cotton and without specimens were also prepared as controls. Two sets of tubes were ready for testing in light and dark. After 18 h incubation at the appropriate temperature, the specimens were removed, and OD_{600} was determined. The antimicrobial activity of the cotton fabrics was evaluated by the reduction in bacterial growth in the presence of the treated specimens compared to the native. The tests were performed in triplicate, and the averages were given (with standard deviations of less than 5%).

2.6. Scanning Electron Microscopy

SEM evaluates adhesion and biofilm formation on the cotton fabric. Tubes containing MPB and samples of untreated and treated cotton fabrics were inoculated with a suspension of *P. aeruginosa* for 24 h, after which the samples were washed with phosphate-buffered saline, dried, and coated with gold using a Jeol JFC-1200 coating apparatus (Leol Ltd.,

Tokyo, Japan) and then examined them at different magnifications by Jeol JSM-5510 SEM (Leol Ltd., Tokyo, Japan).

2.7. Cytotoxicity Assay

Polymers P1–P3 were prepared in various concentrations and diluted in a maintenance medium, with 0.1 mL added to each well of 96-well plates (Costar®, Corning Inc., Kennebunk, ME, USA) containing monolayer cells. These cells were then incubated for 48 h at 37 °C in a humidified atmosphere with 5% CO_2. Following incubation and microscopic examination, the following procedures were performed:

1. The polymer medium was removed, and the cells were thoroughly washed.
2. Each well received 0.1 mL of maintenance medium containing 0.005% neutral red dye.
3. The cells were incubated for 3 h at 37 °C.

After the second incubation, the neutral red dye was aspirated, and the cells were rinsed with PBS. Next, 0.15 mL of a desorb solution (1% glacial acetic acid and 49% ethanol in distilled water) was added to each well. The optical density (OD) at 540 nm was measured using a microplate reader (Biotek Organon, West Chester, PA, USA). The 50% cytotoxic concentration (CC_{50}) was determined as the polymer concentration that reduced cell viability by 50% compared to the untreated control.

The evaluation of the tested compounds' cytotoxicity revealed that compound P1 demonstrated the highest cytotoxicity (CC_{50} = 13.6 μg/mL), followed by the other two, which showed similar ones (P2 CC_{50} = 76 μg mL^{-1} and P3 CC_{50} = 80 μg mL^{-1}).

2.8. Virucidal Assay

We evaluated the virucidal effects of compounds P1, P2, and P3 (irradiated for 1 h and non-irradiated), and treated and untreated fabrics using the following procedure:

1. Identical 1 cm^2 pieces of fabric were cut and immersed in 200 μL of viral suspension containing HAdV5 ($10^{6.0}$ $CCID_{50}$, VR-1516™ ATCC, Manassas, VA, USA) and HRSV-S2 ($10^{5.3}$ $CCID_{50}$, VR-1540™ ATCC, Manassas, VA, USA) for 30 and 60 min, respectively.
2. Non-treated textiles served as controls.
3. After the specified immersion times, the virus suspensions were collected.

Next, HEp-2 cells (ATCC CCL-23™, Manassas, VA, USA) were seeded in 96-well plates (Costar®, Corning Inc., Kennebunk, ME, USA) and incubated at 37 °C with 5% CO_2 for 48 h for HAdV5 and 72 h for HRSV-2. Following incubation and microscopic evaluation, the following steps were performed:

1. The maintenance medium was removed, and the cells were washed.
2. Each well received 0.1 mL of maintenance medium containing 0.005% neutral red dye (N-3246, Invitrogen™, Thermo Fisher Scientific Corporation, St. Bend, OR, USA).
3. The cells were incubated at 37 °C for 3 h.

After incubation, the neutral red dye was removed, and the cells were washed with PBS (20012027, Thermo Fisher Scientific Corporation, St. Bend, OR, USA). Then, 0.15 mL of desorbing solution (1% glacial acetic acid and 49% ethanol in distilled water) was added to each well. The optical density (OD) of the solution was measured at 540 nm using a microplate reader (Biotek Organon, West Chester, PA, USA). The residual infectious virus was quantified using the end-point dilution method, and the Δlogs were calculated by comparing each sample to the control.

3. Results and Discussion

3.1. Hyperbranched Polymers P1–P3

Treatment of Cotton Fabrics with P1–P3 and Their Release from the Cotton Surface

There are various methods for depositing biologically active substances on the surface of cotton materials to produce antimicrobial fabrics that inhibit the growth and spread of pathogenic microorganisms on them. This study used the exhaustion method to deposit the polymers on the cotton fabric. The polymers P1–P3 are insoluble in water but are well soluble in organic solvents such as DMF. For this reason, P1–P3 polymers were initially dissolved in DMF, and then the solution was poured into deionized water. A cotton fabric was immersed in the solution and treated with stirring for three hours at 60 °C; thereafter, the fabric was removed from the bath, washed repeatedly with water and dried. The antimicrobial activity, singlet oxygen generation, and polymer release from the cotton fabric under different conditions were investigated.

The number of polymers adsorbed by the cotton was investigated by the fluorescence intensity ratio in the maximum emission before and after the fabric treatment. It was found that the polymers adsorbed very well on 1 g of cotton surface: 4.30 mg (P1), 4.20 mg (P2) and 4.05 mg (P3), which is 81–86% of the initially used polymers.

Figure 1 shows images of the resulting colorations of cotton materials after treatment with P1–P3 compared with untreated cotton fabric, used as a control when irradiated with sunlight and UV light at 365 nm. The photos show their uniform adsorption on the cotton surface. The control cotton fabric is chemically unbleached and is white. A yellow coloration is obtained when using P1, which absorbs in the visible spectral region, while P3 does not impart color in the treatment due to its absorption in the UV region. When irradiated with monochromatic UV light with λext = 365 nm, due to the emitted fluorescence, the color intensity is enhanced, as for P1, it is yellow-green, for P2, it is blue-green, and for P3, it is blue.

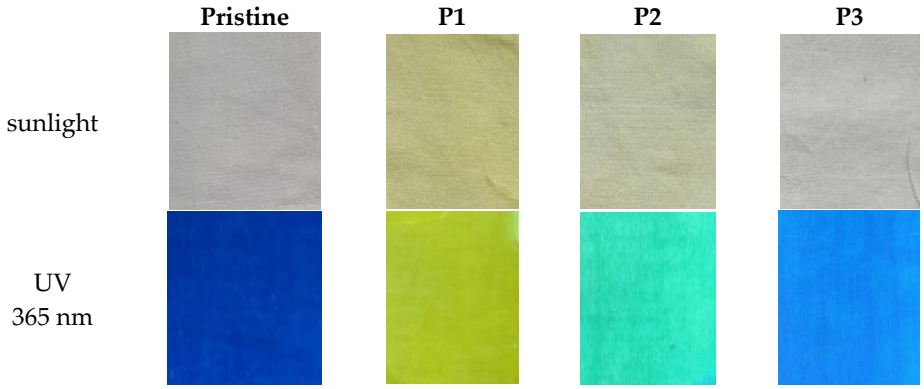


Figure 1. Micrograph of cotton fabrics treated with P1–P3 upon their illumination with sunlight and ultraviolet light at 365 nm.

Table 1 collects the color coordinates L*, a*, b* of the starting fabric and the cotton fabrics treated with polymers P1–P3 before and after washing. It also shows the color difference ΔE* of each treated fabric to pristine cotton fabric, which is used as standard.

Table 1. Color characteristics of cotton fabrics treated with P1-P3 polymers.

	Before Washing				**After Washing**			
Sample	L*	a*	b*	ΔE*	L*	a*	b*	ΔE*
Cotton	83.55	−0.19	1.41	-	83.55	−0.19	1.41	-
Cotton + P1	84.30	−8.76	33.42	33.15	84.24	−7.13	25.83	25.27
Cotton + P2	84.57	−7.98	15.25	15.92	85.53	−7.28	12.95	13.69
Cotton + P3	85.10	−1.00	1.83	1.79	84.86	−0.88	1.69	1.50

L* describes the lightness of the samples, a* refers to the color position between green and red, and b* is the color position between yellow and blue. The results show that the lightness of the obtained fabrics (L*) is greater than that of the untreated cotton fabric due to the fluorescence emitted by the polymers. The color difference ΔE* of P3-treated cotton fabric is too small and cannot be differentiated by the human eye. It has approximately similar values for a* and b* with the untreated fabric but a higher value of L*. The increase in the b* values of the three cotton fabrics in the following order: 1.83 (P3), 15.25 (P2) and 33.42 (P1), corresponds to an increase in the intensity of the yellow color.

The greenish hue is determined by the following values: a* = −7.13 for P1 and a* = −7.28 for P2. Also, the color difference ΔE* shows that the most significant color change occurs when using P1, and an almost minimal difference occurs when using P3. These results are also confirmed by the reflectance curves of the treated cotton fabrics compared to the control fabric when irradiated with a D65 light source, which mimics daylight with an extended UV range. Figure 2 shows that the fluorescence maximum of the P1-treated fabric is at 545 nm, at 471 nm of P2, and at 504 nm of P3. These fluorescence maxima are very close to those of polymers in ethanol solution [23–25]. The slight difference in the positions of the maxima in the solution and on the fabric is due to the firm fixation of the polymers on the fabric and the lack of possibility for rotation of the molecules.

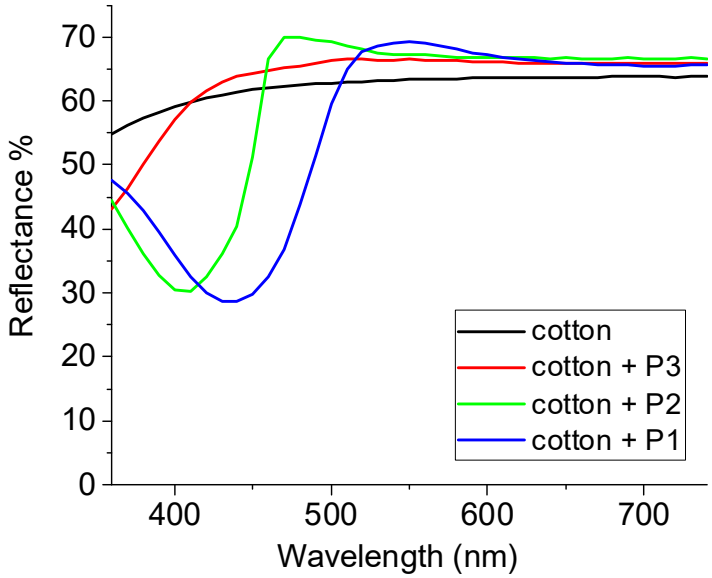


Figure 2. Reflectance curve of cotton fabric and cotton fabric treated with P1–P3.

The retention and stability of P1–P3 on the cotton surface is due to the formation of hydrogen bonds and Van der Waals interactions between the polymers and the textile matrix. The presence of many carbonyl groups (C=O), tertiary and secondary nitrogen atoms, both from the polymer structure and the fluorophores attached to it, favors the formation of hydrogen bonds with many hydroxyl groups from the cellulose cotton structure. On the other hand, the studied polymers P1–P3 are water-insoluble, further complicating their separation and presence in buffer solutions. The stability of the polymers on the cotton surface when treated with a phosphate-buffer solution at pH = 7.4 and acetate buffer pH = 4.5 was studied by fluorescence spectroscopy, monitoring their release for ten hours at 37 °C. Figure 3A shows that only about 4–5% of the adsorbed polymers were separated in the solution for ten hours, which indicates their stable retention on the cotton fabric surface.

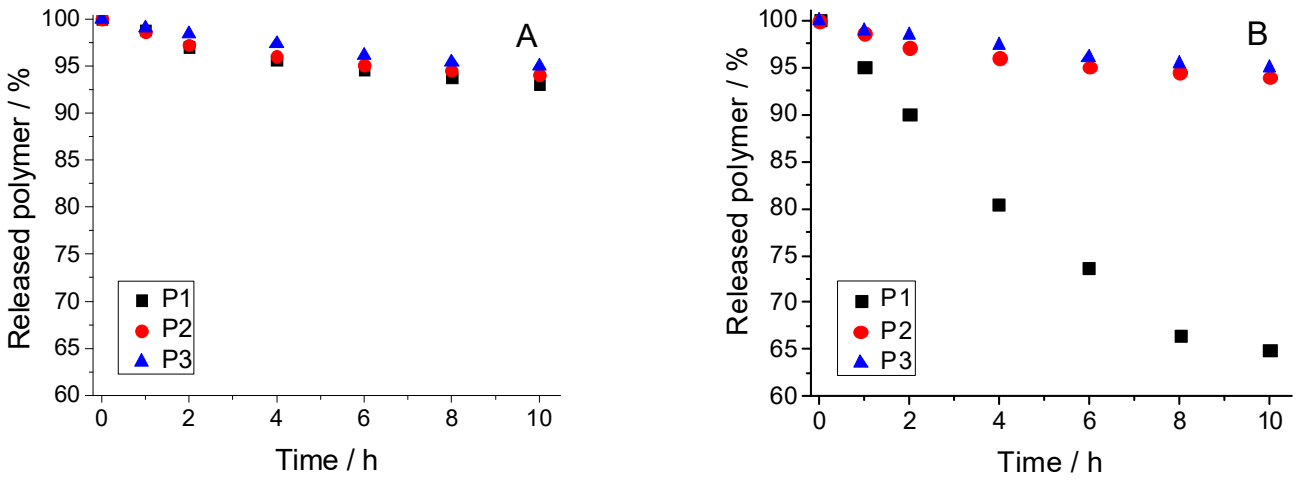


Figure 3. The release of polymers P1, P2, and P3 from the cotton fabric in a phosphate buffer with pH = 7.4 (**A**) and in an acetate buffer with pH = 4.5 (**B**) at 37 °C.

In the acetate buffer (pH = 4.5) of the cotton fabric treated with P1, probably due to the possibility of partial protonation of the *N*,*N*-dimethylamino group (-$NHCH_2CH_2N(CH_3)_2$) from 1,8-naphthalimide units converting it into a water-soluble form, its release from the fabric is significantly better expressed compared to P2 and P3 (Figure 3B).

The color fastness of the treated cotton fabrics to wet processing was tested by ten-fold washing, and the color difference ΔE* was measured (Table 1). The results showed a negligible change, which means excellent fastness and retention of polymers on the cotton surface.

3.2. Generation of Singlet Oxygen

The generation of singlet oxygen ($^1O_2$) during the irradiation of polymers in water (P) ($c = 1 \times 10^{-6}$ mol L^{-1}) and cotton fabrics treated with them has been demonstrated by the iodometric method [28–30]. The process is based on the interaction of singlet oxygen, produced during irradiation, with iodide anions (I^-), which, as a result of photooxidation, is converted into triiodide ions (I_3^-). They have two well-defined maxima in the UV region, unlike (I^-). This allows the production of singlet oxygen to be monitored by absorption spectrometry. The mechanism of formation of (I_3^-) involves five steps.

Figure 4 shows the dependence of the photooxidation of I^- to I_3^- due to the release of singlet oxygen from polymers P1–P3 on the irradiation time. Before irradiation, the solution does not absorb in the spectral range 270–500 nm (Figure 4A). In the absorption spectrum of the KI solution in the presence of polymer P1 given as an example, two well-defined maxima at 288 and 352 nm are registered, which are typical of the formed I_3^- in the solution [28–30]. It is shown that the intensity of the two maxima increases with the irradiation time, which means that the amount of generated singlet oxygen increases. Figure 4B compares the dependence of the absorption at 352 nm as a function of the irradiation time of the three polymers. When comparing the activity of the three polymers, P1 produces a slightly higher amount of $^1O_2$, followed by P2 and the least by P3 (Figure 4B). This can be explained by their different abilities to absorb light from the solar spectrum. In ethanol solution, their absorption maxima are as follows: P1 at 438 nm [23], P2 at 395 nm [24], while P3 absorbs in the UV region at 335 nm [25] (Figure 5).

As a control, the absorption of the solution in the dark was used, as well as that of the irradiated solutions of the polymers without the addition of potassium iodide, in which no absorption of the solutions was recorded, showing that singlet oxygen is not formed.

Light excitation	$P_0 + h\nu \rightarrow {}^1P$
Intersystem crossing	${}^1P \rightarrow {}^3P$
Energy transfer	${}^3P + {}^3O_2 \rightarrow P_0 + {}^1O_2$
Interaction of singlet oxygen with potassium iodide	${}^1O_2 + I^- \rightarrow IOO^- \rightarrow IOOH$
Production of potassium triiodide	$IOOH + I^- \rightarrow HOOI_2^- \rightarrow I_2 + HO_2^- \rightarrow I_3^- + H_2O_2 + OH^-$

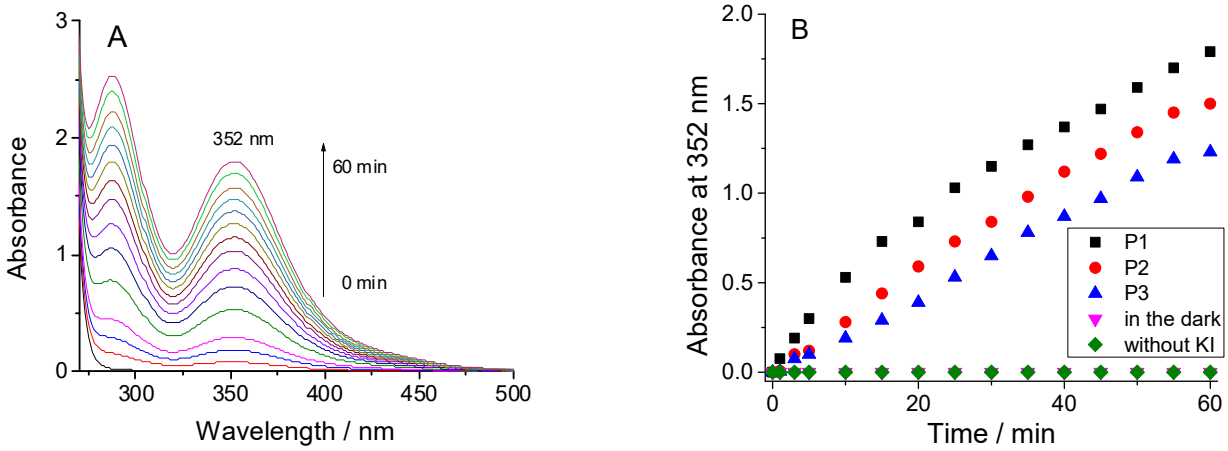


Figure 4. Absorption spectra of 0.5 M KI photo oxidized to I_3^- in the presence of polymer P1 (**A**); dependence of the absorption at 352 nm corresponding to I_3^- caused by polymers P1–P3, polymers in the dark and without KI (**B**), as a function of irradiation time.

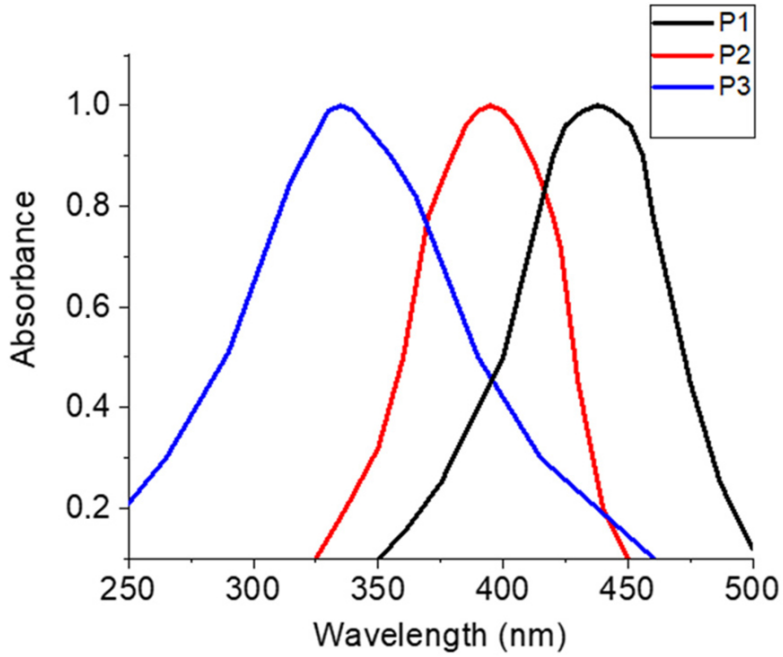


Figure 5. Normalized absorption spectra of polymers P1–P3 in ethanol solution.

Similar studies were conducted using cotton fabric treated with polymers P1–P3 as a function of the irradiation time, whereby the fabric was placed in an aqueous solution of KI. As shown in Figure 6A, the spectral profile of the solution in which the fabric was immersed is the same as when using a solution of polymer P1 as an example. This means that the polymer molecules generate the formation of singlet oxygen, although they are located on the fabric. Figure 6B presents the dependence of the absorption at 352 nm as a function of

irradiation time for polymers P1–P3. A linear relationship is observed, in which case the activity of P1 is also slightly better expressed than that of P2 and P3, which have very close values. These results are similar to those obtained in the polymers' solution, indicating they can generate singlet oxygen in the solid state. As controls, cotton fabrics treated with P1–P3 in KI solution in the dark, irradiated samples in the absence of KI, and untreated cotton fabric in KI solution were used. No absorption was recorded in the studied spectral range in all three cases, meaning no singlet oxygen is generated under these conditions.

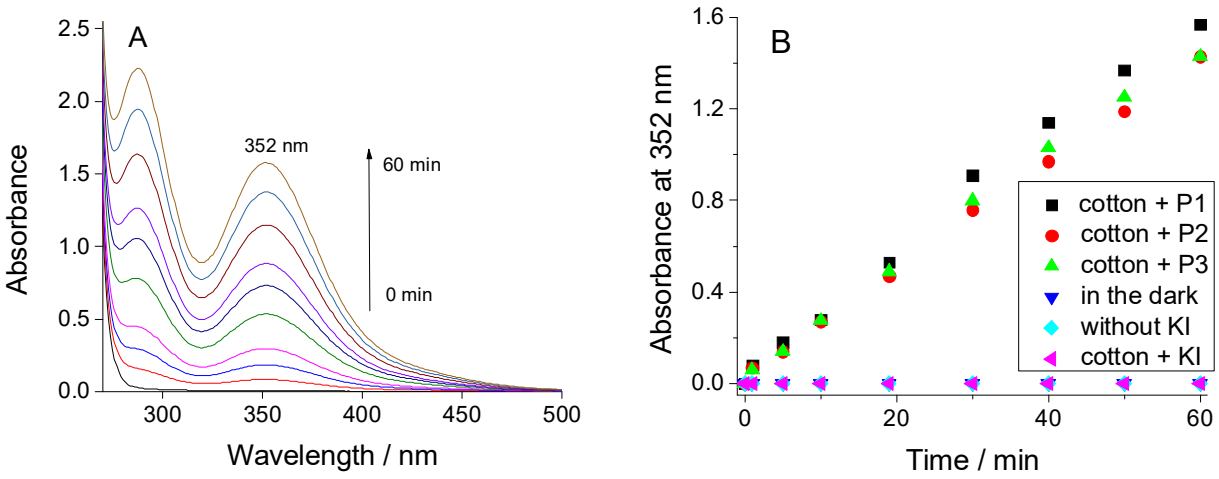


Figure 6. Absorption spectra of 0.5 M KI photooxidized to I_3^- in the presence of cotton fabrics treated with polymer P1 (**A**); dependence of the absorption at 352 nm corresponding to I_3^- caused by cotton fabrics treated with polymers P1–P3, cotton with KI, polymers in the dark and without KI (**B**), as a function of irradiation time.

3.3. The Hydrophilicity of Cotton Fabrics

Due to their hydrophilic nature, products containing cotton materials can retain moisture, which is a suitable environment for developing pathogenic microorganisms such as bacteria, fungi, and viruses. On the other hand, the hydrophobic nature of such items will make it difficult for them to be retained on the surface. To evaluate the hydrophilicity of P1–P3 treated cotton materials, their water adsorption was investigated by statically immersing them in deionized water for 5 min. The amount of water adsorbed was determined by the following formula [31]:

$$\text{Adsorption (\%)} = (\text{mass of water adsorbed}/\text{initial mass}) \times 100. \quad (5)$$

The adsorbed water of the untreated cotton fabric was 114%. After the immobilization of the polymers on the cotton surface, the ability of water molecules to penetrate and retain in the cotton materials was significantly reduced; using P1, the amount of water retained was 87%; for P2, it was 89%; and for P3 it was 90%, respectively. The results show that the polymers increase the hydrophobicity of the cotton fabric, but the type of fluorophore is insignificant. This effect is due to the polymer-induced increase in hydrophobic groups on the surface of the treated cotton fabric, which blocks most of the hydrophilic hydroxyl groups of the cotton.

3.4. The Effect of Light on Bacterial Growth

The main targets in antimicrobial photodynamic therapy are the lipids and proteins of the external structures of pathogen microorganisms, the cytoplasmic membrane, cell walls, capsids, and lipid envelopes. Thus, the induced oxidative stress causes permanent damage to these vital cellular components, leading to the inactivation of pathogenic microbes, and

avoiding the development of photoresist strains. The effect of visible light on the antimicrobial activity of the studied polymers was tested against model Gram-positive *B. cereus* and Gram-negative *P. aeruginosa* bacterial strains. Experiments of P1–P3 were performed in solution and after their application on cotton fabric. The results showed that the polymers could inhibit the growth of the model cultures compared to the negative control. The P1 showed higher antibacterial activity, followed by the P2 and P3 polymers (Figure 7). All three polymers' activity increased after light irradiation, and this effect was better expressed in the case of the Gram-positive strain *B. cereus*. At a concentration of 25 μg/mL, in the dark, P1, P2, and P3 reduced the growth of *B. cereus* by about 57%, 40%, and 23%, respectively. After light irradiation, the growth inhibition increased to about 82%, 68%, and 76%, respectively, compared to the control. In Gram-negative *P. aeruginosa* at the same concentration, a weaker inhibition effect was observed than in *B. cereus*, with inactivation of 37%, 18%, and 13% in the dark and 68%, 58%, and 46% under light irradiation, respectively, when using P1, P2, and P3. The enhanced antimicrobial activity of polymers P1-P3 during light irradiation is attributed to the capability of the fluorophores attached to them to produce reactive singlet oxygen $^1O_2$ when stimulated by light irradiation [20,32,33]. These reactive species attack the outer layer of the bacterial membrane through multi-targeted actions. Thus, oxidative stress causes irreparable damage to bacterial cellular components, leading to their significant inactivation [34].

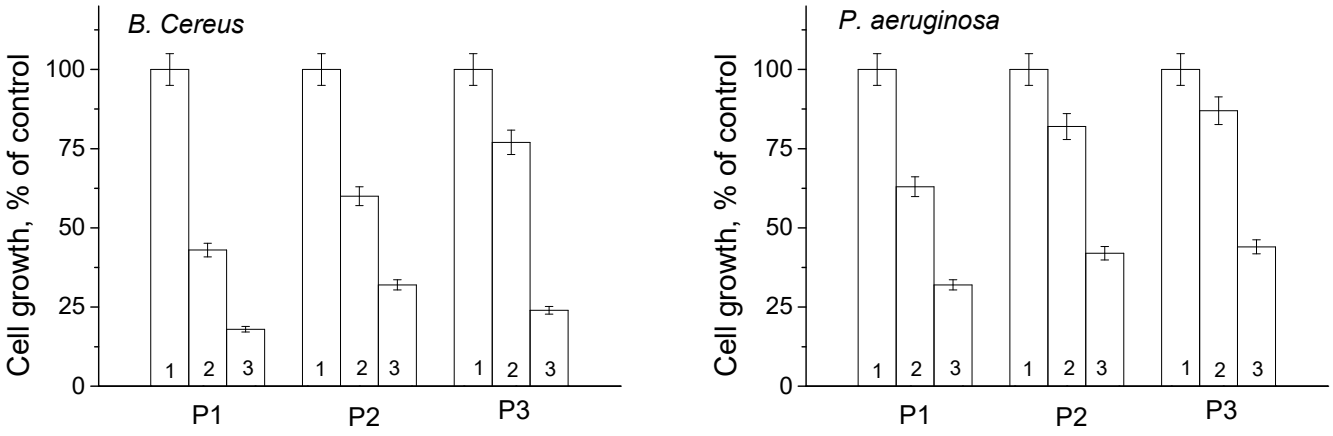


Figure 7. The effect of visible light on model bacteria *P. aeruginosa* and *B. cereus* growth in the presence of P1, P2, and P3 (at a concentration of 25 μg mL^{-1}). (1—control at dark and after illumination, 2—in the dark, and 3—after light illumination).

3.5. Antimicrobial Activity of Modified Cotton Fabrics

Singlet oxygen is essential in various chemical and biological processes, but it can be used for disinfection, including textile materials. It is an oxidant and can attack biomolecules in microbial cells located on the surface of tissues. This leads to the destruction of their cell membranes, proteins and DNA, which causes the death of microorganisms. When singlet oxygen interacts with pathogenic microorganisms on tissues, it can reduce or eliminate their numbers. Bacterial cells are more sensitive to singlet oxygen than human cells, as they lack the complex defense system that human cells have. Through their antioxidant mechanisms, they can mitigate the harmful effects of singlet oxygen.

The antimicrobial activity of cotton fabric treated with polymers P1–P3 was tested in MPB by reducing the growth of model strains. The inhibition of bacterial growth of modified cotton fabrics against both types of bacteria followed the same trend as the polymers, indicating that their activity was maintained after their application to the cotton fabric. As shown in Figure 8, the activity was enhanced after light irradiation, with the best effect observed for polymer P1, followed by P2 and P3, due to the singlet oxygen generated

by the deposited polymers. Their antimicrobial activity against bacteria was investigated also after the tenth wash to clarify the long-term antimicrobial effect of cotton fabrics. The results show a slight decrease in their activity by about 5–8% compared to the first results, which is a good indicator of the fixation and retention of polymers on the cotton fabric and for the use of cotton fabrics as antimicrobial textiles with biomedical applications.

Scanning electron microscopy was used to demonstrate the absence of bacterial biofilm on the surface of cotton fabrics treated with P1–P3. This technique allows us to observe the attachment of bacteria to the surface of materials and the subsequent formation of a stable bacterial biofilm on their surface. It is an arrangement of bacterial cells and their envelopment with a biopolymer polysaccharide matrix produced by them. In this way, they are isolated from external influences such as chemicals and antibiotics. SEM micrographs of virgin cotton fabric (Figure 9A), untreated cotton fabric in contact with *P. aeruginosa* (Figure 9B), cotton fabric treated with P1 in contact with bacteria in the dark (Figure 9C), and during the irradiation with sunlight (D) are presented in Figure 8. Figure 9A displays untreated cotton fabric, revealing the characteristic fibrillar structure of the cotton fibers. The results show the formation of a stable biofilm of *P. aeruginosa* bacteria colonies on a bacterial biopolymer matrix on a cotton surface not treated with P1 (Figure 9B). In the case of the polymer-treated cotton fabric, no biofilm was observed upon contact with the bacteria, but only individual ones were attached to its surface (Figure 9C). When the P1-treated cotton fabric was placed in contact with the bacteria in the light, only single pathogenic cells were observed on the surface of the cotton fabric (Figure 9D). The bacteria's lack of primary microbial adhesion to the cotton surface can be explained by the inability to form a stable bacterial film on the surface of the polymer-treated fabrics. The studied hyperbranched polymers are hydrophobic, and when applied to cotton fabric, they significantly reduce the hydrophilic nature of cotton. In this way, they directly interact with the bacterial cell wall, which changes its properties and prevents microbial retention [35]. This effect is significantly enhanced upon light irradiation due to the synergistic effect caused by the formation of singlet oxygen. The results indicate that cotton fabrics treated with P1–P3 have the property of self-disinfecting. When comparing micrographs 8A and 8D, the microfibrils of the cellulose fiber are preserved, which indicates that singlet oxygen does not significantly affect their structure and mechanical properties. This is due to the fact that singlet oxygen preferentially attacks electron-rich organic molecules, such as those with conjugated double bonds or heteroatoms [36,37].

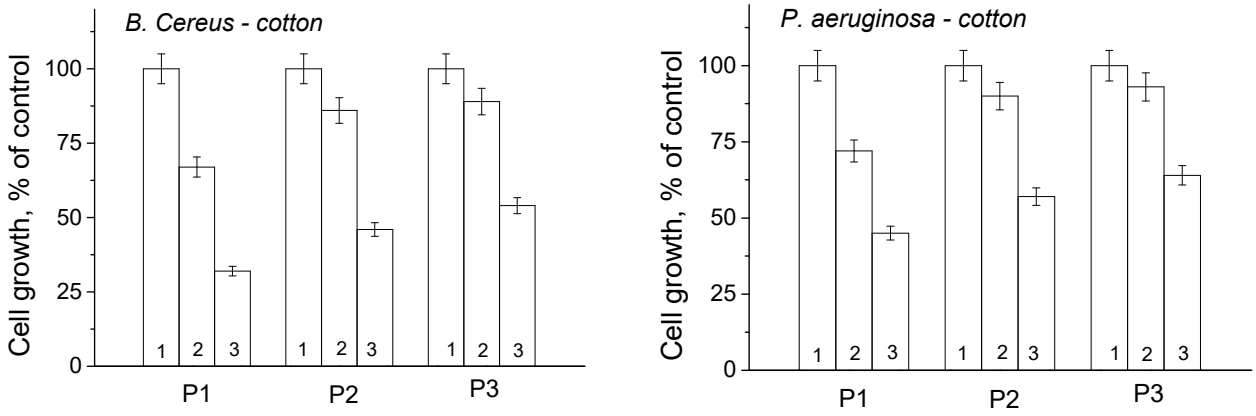


Figure 8. The effect of visible light on the growth of the model strains *P. aeruginosa* and *B. cereus* in the presence of cotton fabrics treated with polymers P1, P2, and P3, (1—control at dark and after illumination, 2—in the dark, and 3—after light illumination).

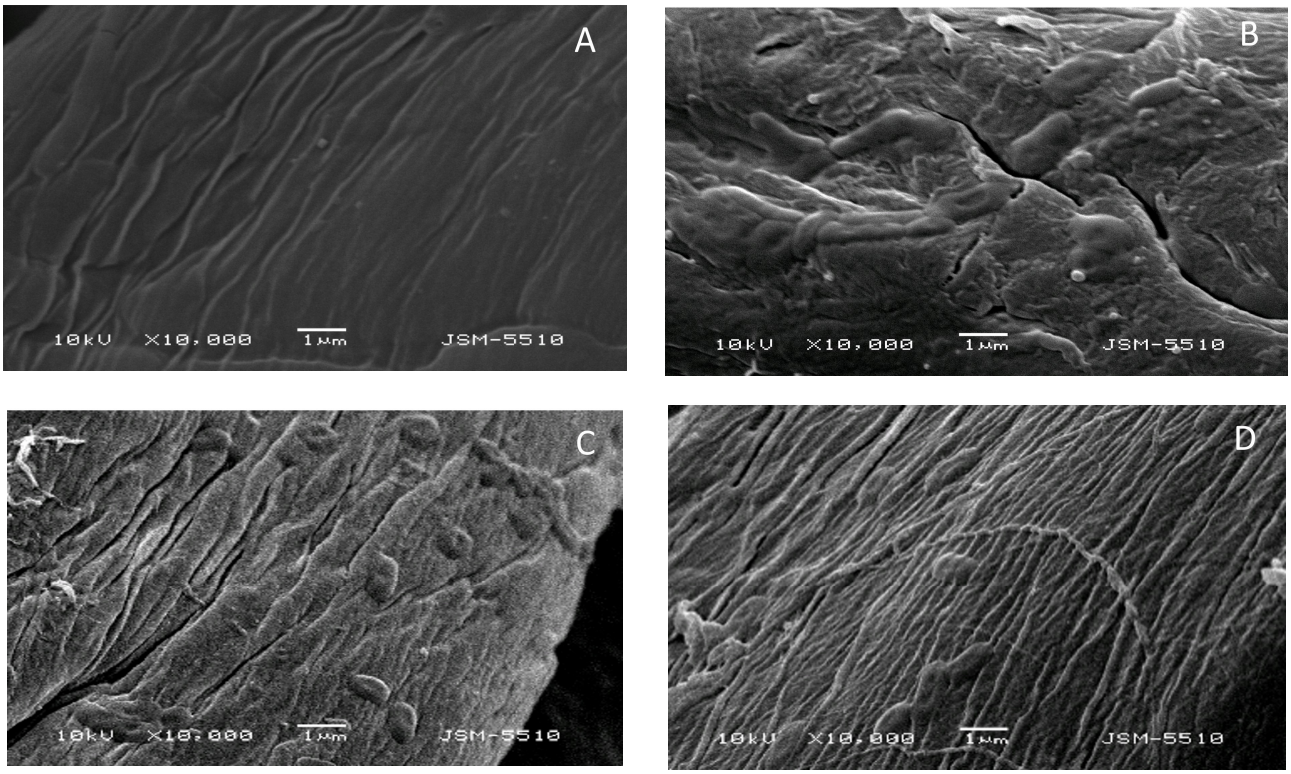


Figure 9. SEM micrographs at 10,000× magnification of untreated cotton fabric (**A**), biofilm of *P. aeruginosa* on untreated cotton fabric (**B**), cotton fabric treated with P1 and in contact with bacteria in the dark (**C**), and cotton fabric treated with P1 in contact with bacteria during sunlight irradiation (**D**).

3.6. Virucidal Activity of Polymers P1–P3

In experiments with non-irradiated substances, no difference in viral titers was observed for the respiratory syncytial virus (HRSV) at 30 and 60 min of contact time. However, after irradiating the compounds for 1 h and a subsequent 60 min contact time with the virus, the titer differences were as follows—Δlog = 0.2 for P1, Δlog = 0.2 for P2 and Δlog = 0.5 for P3 (Table 2). For adenovirus (HAdV), non-irradiated substances showed no change in viral titers at 30 and 60 min of contact time. When the compounds were irradiated for 1 h, with a 60 min contact time, the virus titer was reduced by Δlg = 0.6 for P1, Δlg = 0.3 for P2 and Δlg = 0.9 for P3 (Table 3). Experiments with non-irradiated fabrics treated with the respective compounds showed no change in viral titers for both viruses.

Table 2. Virucidal effect against HRSV-2 and HAdV-5 (irradiated with light for 1 h and non-irradiated).

	HRSV-2				**HAdV-5**			
	Irradiated		**Non-Irradiated**		**Irradiated**		**Non-Irradiated**	
	Δlog 30 min	**Δlog 60 min**	**Δlog 30 min**	**Δlog 60 min**	**Δlog 30 min**	**Δlog 60 min**	**Δlog 30 min**	**Δlog 60 min**
P1	0	0.2	0	0	0	0.6	0	0
P2	0	0.2	0	0	0	0.3	0	0
P3	0	0.5	0	0	0	0.9	0	0

After light irradiation was treated with the compound fabrics, there was no difference in viral titers at a 30 min contact time for both viruses. At a 60 min contact time, the titer differences for HRSV were Δlog = 0.1 for P1, Δlog = 0.1 for P2 and Δlog = 0.3 for P3. For HAdV at a 60 min contact time, the titer differences, respectively, were—Δlg = 0.2 for P1, Δlg = 0.1 for P2 and Δlg = 0.4 for P3.

Table 3. Cotton fabrics treated with the polymers—virucidal effect against (irradiated with light for 1 h and non-irradiated).

	HRSV-2				HAdV-5			
	Irradiated		Non-Irradiated		Irradiated		Non-Irradiated	
	Δlog 30 min	Δlog 60 min	Δlog 30 min	Δlog 60 min	Δlog 30 min	Δlog 60 min	Δlog 30 min	Δlog 60 min
P1	0	0.1	0	0	0	0.2	0	0
P2	0	0.1	0	0	0	0.1	0	0
P3	0	0.3	0	0	0	0.4	0	0

Interestingly, the more stable adenovirus showed greater sensitivity to the compounds and treated cotton fabrics than the respiratory syncytial virus.

4. Conclusions

Three new cotton fabrics with antimicrobial properties were obtained by deposition on the fiber surface of photoactive hyperbranched polymers modified with 1,8-naphthalimide (P1), acridine (P2), and dansyl (P3) fragments. It was found that the release of polymers from cotton fabric occurs slowly at pH = 7.4 whereas in an acidic medium pH = 4.5, due to protonation of the tertiary amino group of 1,8-naphthalimide P1, passes significantly more readily into the aqueous solution.

The in vitro microbiological activity of hyperbranched polymers P1, P2, and P3 and cotton fabrics treated with them was investigated against Gram-negative *P. aeruginosa* and Gram-positive *B. cereus* model bacteria and two respiratory viral strains HRSV-2 and HAdV-5 in the dark and after irradiation with sunlight. The results show high microbiological activity of all three polymers against Gram-positive and Gram-negative bacterial strains, and their activity is preserved after their application to cotton fabric. The antibacterial effect was enhanced several times after irradiation with light due to the singlet oxygen generated by the polymers. In the dark, the microbiological impact of cotton fabrics treated with P1–P3 is mainly due to their contact with microbial cells. On the other hand, the polymers deposited on the cotton fabric prevented the formation of bacterial biofilms. The virucidal effect against respiratory viruses HRSV-2 and AAdV-5 was observed only after irradiation. The results of this study suggest that hyperbranched polymers have promising potential for producing antibacterial and self-disinfecting textiles with biomedical applications. The future validity of this research will be serified through pilot experiments in actual usage conditions.

Author Contributions: Conceptualization, D.S., P.B. and I.G.; methodology, D.S., P.B. and I.G.; formal analysis, P.B., P.G. and I.N.; investigation, P.B., P.G. and I.N., writing—original draft preparations, D.S. and I.G., writing—review and editing, I.G. and D.S.; visualization, I.G.; project administration, D.S., I.G. and P.B. All authors have read and agreed to the published version of the manuscript.

Funding: This study was financed by the European Union Next Generation EU through the National Recovery and Resilience Plan of the Republic of Bulgaria, project № BG-RRP-2.004-0008, and the European Union's NextGenerationEU package through the National Recovery and Resilience Plan of the Republic of Bulgaria, project № BG-RRP-2.004-0002, and the "BiOrgaMCT" of the European Union (NextGenerationEU) through the CSIC Interdisciplinary Thematic Platform Salud Global+ (PTI-SALUDGLOBAL+).

Data Availability Statement: No new data were created.

Conflicts of Interest: The authors declare no conflicts of interest.

References

1. Meade, E.; Slattery, M.A.; Garvey, M. Biocidal Resistance in Clinically Relevant Microbial Species: A Major Public Health Risk. *Pathogens* **2021**, *10*, 598. [CrossRef]
2. Gauba, A.; Rahman, K.M. Evaluation of Antibiotic Resistance Mechanisms in Gram-Negative Bacteria. *Antibiotics* **2023**, *12*, 1590. [CrossRef]
3. Uddin, T.M.; Chakraborty, A.J.; Khusro, A.; Zidan, B.M.R.M.; Mitra, S.; Emran, T.B.; Koirala, N. Antibiotic resistance in microbes: History, mechanisms, therapeutic strategies and prospects. *J. Infect. Public Health* **2021**, *14*, 1750–1766. [CrossRef]
4. De Oliveira, D.M.P.; Forde, B.M.; Kidd, T.J.; Harris, P.N.A.; Schembri, M.A.; Beatson, S.A.; Paterson, D.L.; Walker, M.J. Antimicrobial Resistance in ESKAPE Pathogens. *Clin. Microbiol. Rev.* **2020**, *33*, 10–1128. [CrossRef]
5. World Health Organization. WHO Bacterial Priority Pathogens List, 2024: Bacterial Pathogens of Public Health Importance to Guide Research, Development and Strategies to Prevent and Control Antimicrobial Resistance. Available online: https://iris.who.int/bitstream/handle/10665/376776/9789240093461-eng.pdf?sequence=1 (accessed on 25 November 2024).
6. Mesquita, M.Q.; Dias, C.J.; Neves, M.G.P.M.S.; Almeida, A.; Faustino, M.A.F. Revisiting Current Photoactive Materials for Antimicrobial Photodynamic Therapy. *Molecules* **2018**, *23*, 2424. [CrossRef]
7. Schmidt, R. Photosensitized generation of singlet oxygen. *Photochem. Photobiol.* **2006**, *82*, 1161–1177. [CrossRef]
8. Warrier, A.; Mazumder, N.; Prabhu, S.; Satyamoorthy, K.; Murali, T.S. Photodynamic therapy to control microbial biofilms. *Photodiagnosis Photodyn. Ther.* **2021**, *33*, 102090. [CrossRef]
9. Yu, Y.; Jia, H.; Liu, Y.; Zhang, L.; Feng, G.; Tang, B.Z. Recent Progress in Type I Aggregation-Induced Emission Photosensitizers for Photodynamic Therapy. *Molecules* **2023**, *28*, 332. [CrossRef]
10. Fleming, D.; Rumbaugh, K.P. Approaches to Dispersing Medical Biofilms. *Microorganisms* **2017**, *5*, 15. [CrossRef]
11. Kalia, V.C.; Patel, S.K.S.; Lee, J.-K. Bacterial biofilm inhibitors: An overview. *Ecotoxicol. Environ. Saf.* **2023**, *264*, 115389. [CrossRef]
12. Efimov, A.; Mordon, S. Photoantimicrobial and Photoantiviral Textiles: Underestimated Potential. *Pharmaceuticals* **2024**, *17*, 1164. [CrossRef]
13. Ghorbani, J.; Rahban, D.; Aghamiri, S.; Teymouri, A.; Bahador, A. Photosensitizers in antibacterial photodynamic therapy: An overview. *Laser Ther.* **2018**, *27*, 293–302. [CrossRef]
14. Mariewskaya, K.A.; Tyurin, A.P.; Chistov, A.A.; Korshun, V.A.; Alferova, V.A.; Ustinov, A.V. Photosensitizing Antivirals. *Molecules* **2021**, *26*, 3971. [CrossRef]
15. Wiehe, A.; O'Brien, J.M.; Senge, M.O. Trends and targets in antiviral phototherapy. *Photochem. Photobiol. Sci.* **2019**, *18*, 2565–2612. [CrossRef]
16. Čuk, N.; Simončič, B.; Fink, R.; Tomšič, B. Bacterial Adhesion to Natural and Synthetic Fibre-Forming Polymers: Influence of Material Properties. *Polymers* **2024**, *16*, 2409. [CrossRef]
17. Gulati, R.; Sharma, S.; Sharma, R.K. Antimicrobial textile: Recent developments and functional perspective. *Polym. Bull.* **2022**, *79*, 5747–5771. [CrossRef]
18. Grabchev, I.; Vasileva-Tonkova, E.; Staneva, D.; Bosch, P.; Kukeva, R.; Stoyanova, R. Impact of Cu(II) and Zn(II) ions on the functional properties of new PAMAM metallodendrimers. *New J. Chem.* **2018**, *42*, 7853–7862. [CrossRef]
19. Grabchev, I.; Vasileva-Tonkova, E.; Staneva, D.; Bosch, P.; Kukeva, R.; Stoyanova, R. Synthesis, spectral characterization, and in vitro antimicrobial activity in liquid medium and applied on cotton fabric of a new PAMAM metallodendrimer. *Int. J. Polym. Anal. Charact.* **2018**, *23*, 45–57. [CrossRef]
20. Manov, H.; Staneva, D.; Vasileva-Tonkova, E.; Grozdanov, P.; Nikolova, I.; Stoyanov, S.; Grabchev, I. Photosensitive dendrimers as a good alternative to antimicrobial photodynamic therapy of Gram-negative bacteria. *J. Photochem. Photobiol. A Chem.* **2021**, *419*, 113480. [CrossRef]
21. Said, A.I.; Staneva, D.; Vasileva-Tonkova, E.; Grozdanov, P.; Nikolova, I.; Stoyanova, R.; Jordanova, A.; Grabchev, I. Synthesis, Spectral Characteristics, Sensing Properties and Microbiological Activity of New Water-Soluble 4-Sulfo-1,8-naphthalimides. *Chemosensors* **2024**, *12*, 79. [CrossRef]
22. Staneva, D.; Atanasova, D.; Nenova, A.; Vasileva-Tonkova, E.; Grabchev, I. Cotton Fabric Modified with a PAMAM Dendrimer with Encapsulated Copper Nanoparticles: Antimicrobial Activity. *Materials* **2021**, *14*, 7832. [CrossRef] [PubMed]
23. Medel, S.; Bosch, P.; Grabchev, I.; de la Torre, M.C.; Ramírez, P. Click chemistry to fluorescent hyperbranched polymeric sensors. 2. Synthesis, spectroscopic and cation-sensing properties of new green fluorescent 1,8-naphthalimides. *Eur. Polym. J.* **2016**, *74*, 241–255. [CrossRef]
24. Medel, S.; Bosch, P.; de la Torre, C.; Ramírez, P. Click chemistry to fluorescent hyperbranched polymers.1—Synthesis, characterization and spectroscopic properties. *Eur. Polym. J.* **2014**, *59*, 290–301. [CrossRef]
25. Medel, S.; Martínez-Campos, E.; Acitores, D.; Vassileva-Tonkova, E.; Grabchev, I.; Bosch, P. Synthesis and spectroscopic properties of a new fluorescent acridine hyperbranched polymer: Applications to acid sensing and as an antimicrobial agent. *Eur. Polym. J.* **2018**, *102*, 19–28. [CrossRef]

26. Bosch, P.; Staneva, D.; Vasileva-Tonkova, E.; Grozdanov, P.; Nikolova, I.; Kukeva, R.; Stoyanova, R.; Grabchev, I. Hyperbranched Polymers Modified with Dansyl Units and Their Cu(II) Complexes. Bioactivity Studies. *Materials* **2020**, *13*, 4574. [CrossRef]
27. Vasileva-Tonkova, E.; Grozdanov, P.; Nikolova, I.; Staneva, D.; Bosch, P.; Medel, S.; Grabchev, I. Evaluation of antimicrobial, biofilm inhibitory and cytotoxic activities of a new hiperbranched polymer modified with 1,8-naphthalimide units. *Bioint. Res. Appl. Chem.* **2018**, *8*, 3053–3059.
28. Mosinger, J.; Mosinger, B. Photodynamic sensitizers assay: Rapid and sensitive iodometric measurement. *Experientia* **1995**, *51*, 106–109. [CrossRef]
29. Wan, L.; Yiming, X. Iodine-sensitized oxidation of ferrous ions under UV and visible light: The influencing factors and reaction mechanism. *Photochem. Photobiol. Sci.* **2013**, *12*, 2084–2088. [CrossRef]
30. Wang, T.; Chen, W.; Dong, T.; Lv, Z.; Zheng, S.; Cao, X.; Wei, Q.; Ghiladi, R.A.; Wang, Q. Color-Variable Photodynamic Antimicrobial Wool/Acrylic Blended Fabrics. *Materials* **2020**, *13*, 4141. [CrossRef]
31. Vaideki, K.; Jayakumar, S.; Rajendran, R.; Thilagavathi, G. Investigation on the effect of RF plasma and neem leaf extract treatment on the surface modification and antimicrobial activity of cotton fabric. *Appl. Surf. Sci.* **2008**, *254*, 2472–2478. [CrossRef]
32. Davi, L.B.O.; Silva, M.S.; Ferreira, R.L.; Muniz, W., Jr.; Ribeiro, A.S.; Lima, D.J.P.; de Oliveira, I.N.; Barbosa, C.D.A.E.S. Multi-functional carbon dots derived from dansyl chloride for ratiometric thermal sensor and reactive oxygen generation. *Dye. Pigm.* **2021**, *194*, 109549. [CrossRef]
33. Fornaciari, B.; Juvenal, M.S.; Martins, W.K.; Junqueira, H.C.; Baptista, M.S. Photodynamic Activity of Acridine Orange in Keratinocytes under Blue Light Irradiation. *Photochem* **2023**, *3*, 209–226. [CrossRef]
34. Almeida, A.; Faustino, M.A.F.; Tomé, J.P.C. Photodynamic inactivation of bacteria: Finding the effective targets. *Future Med. Chem.* **2015**, *7*, 1221–1224. [CrossRef]
35. Sperandio, F.F.; Huang, Y.-Y.; Hamblin, M.R. Antimicrobial photodynamic therapy to kill Gram-negative bacteria. *Recent Pat. Antiinfect. Drug Discov.* **2013**, *8*, 108–120. [CrossRef]
36. Schweitzer, C.; Schmidt, R. Physical mechanisms of generation and deactivation of singlet oxygen. *Chem. Rev.* **2003**, *103*, 1685–1758. [CrossRef]
37. Curieses Andrés, C.M.; Pérez de Lastra, J.M.; Andrés Juan, C.; Plou Gasca, F.J.; Pérez-Lebeña, E. Reactivity and Applications of Singlet Oxygen Molecule [Internet]. In *Reactive Oxygen Species-Advances and Developments*; IntechOpen: London, UK, 2024. [CrossRef]

Disclaimer/Publisher's Note: The statements, opinions and data contained in all publications are solely those of the individual author(s) and contributor(s) and not of MDPI and/or the editor(s). MDPI and/or the editor(s) disclaim responsibility for any injury to people or property resulting from any ideas, methods, instructions or products referred to in the content.